Available online at www.sciencedirect.com
SCIENCE DIRECT
Journal of Molecular Catalysis A: Chemical 235 (2005) 200–208
JOURNAL OF MOLECULAR CATALYSIS A: CHEMICAL
www.elsevier.com/locate/molcata

Post-synthesis alumination of mesoporous silica SBA-15 with high framework aluminum content using ammonium hexafluoroaluminate

Hsien-Ming Kao *, Chun-Chiang Ting, Shih-Wei Chao

Department of Chemistry, National Central University, Chung-Li, Taiwan 32054, ROC

Received 27 September 2004; received in revised form 16 March 2005; accepted 16 March 2005
Available online 10 May 2005

Abstract

Incorporation of high aluminum contents into the silica framework of SBA-15 was achieved by treating SBA-15 with an aqueous $(NH_4)_3AlF_6$ solution at room temperature under alkaline conditions. Characterization by powder X-ray diffraction (XRD), N_2 adsorption–desorption, transmission electron microscopy (TEM), FTIR, and multinuclear solid-state NMR measurements was carried out to evaluate the efficiency of this alumination method. ^{27}Al magic angle spinning (MAS), ^{1}H/^{27}Al TRAnsfer of Population in DOuble Resonance (TRAPDOR) NMR, and cumene cracking measurements demonstrated that the aluminated SBA-15 materials contained exclusively tetrahedrally coordinated aluminum and exhibited well-developed Brønsted acidity. A high level of framework aluminum substitution, up to an Si/Al ratio near 5, without any significant loss in the textural properties of SBA-15, was achieved via the present post-synthesis route. ^{19}F MAS NMR was helpful in gaining more insights into the mechanism of the present alumination process.
© 2005 Elsevier B.V. All rights reserved.

Keywords: Solid-state NMR; Post-synthesis alumination; Brønsted acidity; SBA-15

1. Introduction

The discovery of ordered mesoporous molecular sieves has stimulated extensive research due to the potential use of these materials as versatile catalysts for the conversion of large molecules [1,2]. In particular, incorporation of aluminum into mesoporous materials is of tremendous interest as it gives rise to materials with Brønsted acidity. Extensive efforts have been devoted for maximizing the amount of aluminum that can be tetrahedrally incorporated into mesoporous silicas such as MCM-41 via direct synthesis and post-synthesis methods [3–7]. SBA-15, a mesoporous material synthesized with the triblock copolymer Pluronic P123 as the surfactant under strongly acidic conditions, exhibits a larger pore size and a thicker pore wall than the M41S materials. The improved hydrothermal and thermal stability of SBA-15 make it a more promising catalytic material. Unlike MCM-41 and MCM-48 mesostructures, which are assembled under basic conditions, the SBA-15 mesostructure requires a strongly acidic reaction condition for assembly, which is not very favorable for the direct incorporation of aluminum into the SBA-15 framework. This is because aluminum sources exist only in the cationic form under such acidic conditions, rather than their corresponding oxo species, and therefore cannot be easily introduced into the mesoporous walls via a condensation process with silicon species. Up to now, only a few studies on the direct synthesis of aluminum-containing SBA-15 (designated as Al-SBA-15) have been reported [8–10]. For example, Yue et al. have synthesized Al-SBA-15 by changing the synthesis condition from a strongly acidic condition (pH < 0) to a pH value of 1.5 [8]. However, such aluminum incorporation was not efficient because a large proportion of extra framework aluminum species was observed by ^{27}Al NMR. More recently, a more effective direct synthesis method, so called “pH adjusting method” [9], has been reported. The pH adjusting method involves a two-step approach, in which the conventional low

* Corresponding author. Tel.: +886 3 4275054; fax: +886 3 4227664.
E-mail address: hmkao@cc.ncu.edu.tw (H.-M. Kao).

1381-1169/$ – see front matter © 2005 Elsevier B.V. All rights reserved.
doi:10.1016/j.molcata.2005.03.026

pH of the sol–gel reaction was adjusted up to neutral (pH 7.5) for further crystallization. Compared to other direct synthesis methods, the pH adjusting method could introduce more Al into mesoporous silicas. However, the synthesis procedures were relatively complicated. Later, Li et al. made use of this method combined with a hydrolysis-controlled approach to prepare Al-SBA-15 with the Si/Al ratios in the range of 22–53 [10].

Recently, a novel method using preformed zeolitic nanocluster precursors for the incorporation of heteroatoms into the mesoporous silica synthesized in strongly acidic media has been reported by Xiao and co-workers [11] and Liu and Pinnavaia [12]. The aluminum atom was first incorporated into the framework of the preformed zeolitic nanoclusters and then directly introduced into the mesostructure through the assembly with the surfactant. Although the materials obtained showed high catalytic activity, the aluminum content in these materials was still relatively low. When the Si/Al ratio in the initial gel for MAS-9 was 40, for example, the Si/Al ratio was only 89 in the final product [11].

As described above, the direct synthesis of Al-SBA-15 is difficult and often not stoichiometric. In addition, it often requires specialized synthesis conditions and complicated procedures. From this viewpoint, therefore, the development of a simple post-synthesis method for the alumination of the mesoporous silicas that are synthesized under strongly acidic conditions becomes an appealing alternate choice. In comparison to MCM-41 and MCM-48, however, relatively few post-synthesis alumination methods for SBA-15 have been reported in the literature [13–15]. Most of post-synthesis methods involve the use of aluminum isopropoxide, $Al(CH_3)_3$ and $AlCl_3$ as the aluminum sources, and thus have to be carried out in non-aqueous media in order to avoid the undesirable effect of water. Another disadvantage of these post-synthesis methods is that the ordered mesostructures are sometimes severely destroyed, especially at high aluminum loadings. Moreover, not all the aluminum atoms introduced are located in four-coordinated environments. A significant amount of extra framework aluminum species in the products is usually observed. By using different aluminum sources, Luan et al. concluded that the alumination method using an aqueous sodium aluminate was the most effective [14]. However, only the sample with an Si/Al ratio of 20 was made with sodium aluminate as the aluminum source.

Herein, we present an easy and efficient post-synthesis alumination method for SBA-15 using an aqueous $(NH_4)_3AlF_6$ solution as the aluminum source. This alumination method was first reported by Chang et al. for the incorporation of Al^{3+} into the high silica ZSM-5 framework [16]. The Al-SBA-15 material thus obtained exhibits a high framework aluminum content (up to a bulk Si/Al ratio near 5), good structural integrity, and well-developed Brønsted acidity. To the best of our knowledge, such a high level of Al substitution, without any significant loss in the textural properties of SBA-15, has not been reported so far by post-synthesis methods.

2. Experimental

2.1. Post-synthesis alumination of SBA-15

The pure silica SBA-15 material, denoted as Si-SBA-15, was synthesized according to a previously published procedure [2]. Typically, 4.0 g of Pluronic P123, $EO_{20}PO_{70}EO_{20}$, triblock copolymer was dissolved in 30 g of distilled water. A 2 M HCl (120 g) solution was slowly added into the solution. Then, 8.50 g of tetraethyl orthosilicate (TEOS) was added, and the resulting mixture was stirred for 20 h at room temperature. The mixture was then kept at 90 °C in an oil bath for 1 day. The solid product was filtered, washed with water, and dried in an oven. The Si-SBA-15 sample obtained was then calcined at 560 °C for 8 h to remove the organic templates.

Alumination of SBA-15 was conducted at room temperature by stirring 0.5 g of calcined Si-SBA-15 with 3.0 M $NH_4OH_{(aq)}$ to achieve a pH value of 9.3 in the solution. A 0.02 M aqueous $(NH_4)_3AlF_6$ solution with various volumes was then dropwisely added over a period of 1–3 h. The resulting solution was kept at room temperature for 18 h with constant stirring. The solid product was filtered, washed with cold water, and dried in an oven at 120 °C overnight. These aluminated samples were labeled as *x*-Al-SBA-15, where *x* represents the Si/Al ratio corresponding to the chemical stoichiometric composition in the post-synthesis mixtures.

2.2. Characterization

Elemental compositions of the *x*-Al-SBA-15 samples were determined by inductively coupled plasma–atomic emission spectroscopy (ICP–AES). Small-angle powder X-ray diffraction (XRD) patterns were collected on Wiggler-A beamline ($\lambda = 0.1326$ nm) at the National Synchrotron Radiation Research Center in Taiwan (1.85 GeV and 200 mA). N_2 adsorption–desorption measurements were carried out on a Micromeritics ASAP 2010 system at 77 K with samples outgassed at 180 °C under high vacuum for 1 day. The Brunauer–Emmett–Teller (BET) specific surface area was evaluated using the adsorption data in a relative pressure range from 0.04 to 0.2. The total pore volume was estimated from the amount adsorbed at a relative pressure of about 0.99. The pore size distribution was obtained from the analysis of the adsorption branch of the isotherm by the Barrett–Joyner–Halenda (BJH) method. Transmission electron microscopic (TEM) images were taken from ultrathin sections (~90 nm) of epoxy resin-embedded samples using a Philips Tecnai G2 F20 FEG-TEM instrument.

^{27}Al magic angle spinning (MAS) NMR spectra were recorded on a Bruker DSX-300 spectrometer equipped with a 4 mm MAS probe with a resonance frequency of 78.17 MHz for ^{27}Al nucleus. In order to favor a symmetric environment around the aluminum nucleus, all samples were hydrated under atmospheric moisture conditions before acquiring the

spectrum. All ^{27}Al MAS NMR spectra were obtained with small flip angles of approximately 15° and with a recycle delay of 1 s. ^{19}F MAS NMR spectra were acquired on a Varian Infinityplus-400 with a resonance frequency of 376.31 MHz for ^{19}F nucleus. A $\pi/2$ pulse of 4.5 μs, a recycle delay of 15 s and a spinning speed of 20 kHz were used to acquire the spectrum using a 3.2 mm probe. A Hahn echo sequence was used for refocusing the magnetization lost in the dead time and the signal distorted by the probe. The samples for ^{19}F MAS NMR measurements were obtained by washing the aluminated samples with cold water (0.5 g/100 mL). The ^{19}F and ^{27}Al chemical shifts were externally referenced to $CFCl_3$ and $Al(H_2O)_6^{3+}$ at 0.0 ppm, respectively.

For ^{1}H/^{27}Al TRAnsfer of Population in DOuble Resonance (TRAPDOR) NMR experiments [17], a spin echo pulse was applied to the ^{1}H channel with simultaneous irradiation of aluminum (on-resonance) during the first period of evolution time (τ). An ^{27}Al irradiation field of 50 kHz was used. The sample was dehydrated at 300 °C for 12 h under vacuum and packed into a ZrO_2 rotor in a glove box under N_2 atmosphere before ^{1}H/^{27}Al TRAPDOR NMR measurements. Typically, a $\pi/2$ pulse width of 4 μs and a repetition times of 2 s were used for ^{1}H/^{27}Al TRAPDOR NMR experiments. ^{1}H chemical shifts were quoted relative to tetramethylsilane (TMS) at 0.0 ppm. More detailed theoretical description of the TRAPDOR NMR experiment and some applications can be found in Ref. [18,19].

FTIR spectra of pyridine adsorbed on the Al-SBA-15 samples were recorded on a Bomem DA-8 FTIR spectrometer with a resolution of 0.48 cm^{-1}. The samples were made into self-supporting wafers and were evacuated in an IR cell at 300 °C for 1.5 h before pyridine adsorption. In the pyridine adsorption process, 1 Torr of pyridine was introduced into the IR cell at 150 °C for 0.5 h. FTIR spectra of pyridine adsorbed on Al-SBA-15 were then measured after degassing at each evacuation temperature (in the range 30–500 °C) for 0.5 h. Reference spectra of the unloaded Al-SBA-15 were also recorded. The spectra of pyridine-loaded samples were then corrected by the corresponding reference spectra, and the resulting difference spectra were displayed.

2.3. Catalytic testing

Cumene cracking reaction was performed in a continuous-flow fixed bed reactor (quartz) system with N_2 (40 mL min^{-1}) as the carrier gas and a catalyst loading of 100 mg. The catalyst was pre-treated in flowing nitrogen at 500 °C for 1.5 h and the cumene cracking reaction was performed at 300 °C. Cumene was introduced by passing nitrogen through liquid cumene at 25 °C. The partial pressure of cumene was 4.6 Torr. The weight hourly space velocity (WHSV) was maintained at 1.2 h^{-1}. The products were analyzed by an on-line gas chromatographic system equipped with a flame ionization detector. Cumene conversions were measured after 0.5 h on stream at 300 °C.

3. Results and discussion

3.1. Elemental analysis and XRD

The elemental analysis results, determined by ICP, are listed in Table 1. The Si/Al ratios of the Al-SBA-15 materials are in relatively good agreement with the composition in the post-synthesis mixtures in the range of 5–30. The actual Si/Al ratios of both 15-Al-SBA-15 and 30-Al-SBA-15 were lower than those in the initial synthesis mixture. Thus, a slight loss of silica might have happened via the present synthesis route since the alumination was performed with the liquor at a pH value close to 9. It is notable that the Si/Al ratio is up to 5.3 for the 5-Al-SBA-15 sample (Table 1), which is the highest framework aluminum content incorporated in SBA-15 as compared with other reported post-synthesis alumination methods [13–15]. This Si/Al ratio is also comparable to the recently reported direct synthesis method of pH adjustment [9]. Overall, the Al incorporation via the present post-synthesis method is very efficient.

Fig. 1 shows the small-angle powder X-ray diffraction patterns of Si-SBA-15 before and after post-synthesis alumination. All XRD patterns show a well-resolved pattern with a prominent peak at $2\theta = 0.8°$ and two small peaks at $2\theta = 1.4°$ and 1.6°, which can be indexed to (1 0 0), (1 1 0) and (2 1 0) diffraction peaks, consistent with the pattern reported for SBA-15 [2]. The XRD diffraction peaks can be indexed to a hexagonal lattice with a d_{100} spacing of 9.5 nm, corresponding to a unit cell parameter a_0 of 11.0 nm, based on the formula $a_0 = 2d_{100}/\sqrt{3}$. The well-defined XRD patterns reveal that all samples retain the characteristic patterns of the hexagonal mesostructures after alumination.

Table 1
Elemental composition, textural properties, and catalytic activities of the samples studied

Sample	(Si/Al)[a]	BET (m^2 g^{-1})	Pore volume (cm^3 g^{-1})	Pore size (nm)[b]	Cumene conversion (%)[c]
Si-SBA-15	∞	820	1.07	6.6	0
30-Al-SBA-15	24.8	770	0.97	6.8	26
15-Al-SBA-15	12.5	725	0.87	6.5	39
5-Al-SBA-15	5.3	620	0.72	7.0	55

[a] Determined by ICP.
[b] Determined using the BJH method.
[c] Reaction conditions: catalyst, 0.1 g; temperature, 300 °C; time on stream, 0.5 h.

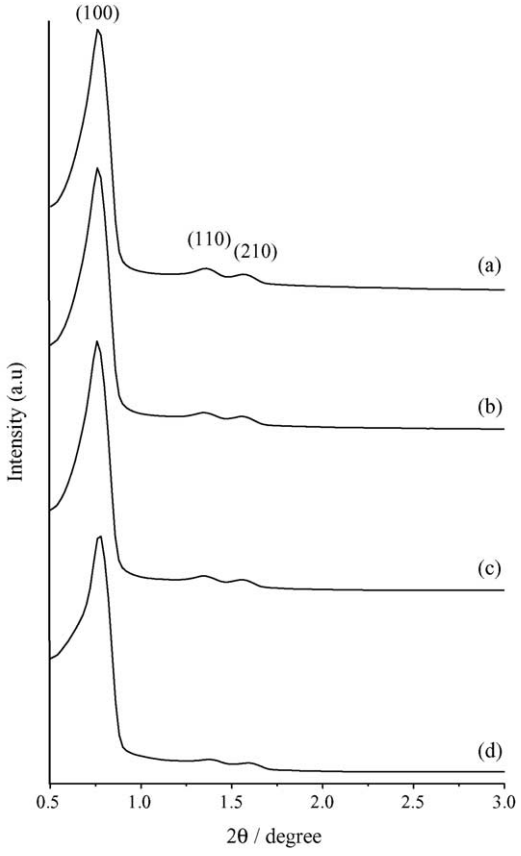

Fig. 1. Powder X-ray diffraction patterns of: (a) Si-SBA-15 and *x*-Al-SBA-15, where *x* = (b) 30, (c) 15 and (d) 5.

3.2. N_2 adsorption–desorption and TEM measurements

Fig. 2 shows the N_2 adsorption–desorption isotherms of the samples studied. Table 1 gives the textural properties of Al-SBA-15 with different Si/Al ratios, together with the data of Si-SBA-15 for comparison. The isotherm is typical of type IV with a clear H1-type hysteresis loop at a high relative pressure, suggesting that Al-SBA-15 possesses very regular mesoporous channels. A well-defined step occurs at a high relative pressure range of 0.6–0.8, corresponding to the capillary condensation in the mesopores, indicative of the uniformity of the pores. The BET specific surface areas and the pore volumes of the Al-SBA-15 samples decreased with increasing Al loadings. The reduction in the surface area and in the pore volume of the Al-SBA-15 samples, as compared to those of pure silica Si-SBA-15, might be due to the partial degradation of the pore structures induced by alkaline dissociation, since the alumination was performed in basic media. Although the pore diameter slightly increased as the aluminum was incorporated, there seemed no direct relationship between this property and the Al contents.

Fig. 3 shows the TEM images of 15-Al-SBA-15. The TEM images showed well-ordered hexagonal arrays of one-dimensional mesoporous channels and confirmed that the sample exhibited a two-dimensional hexagonal structure [2]. The distance between two consecutive centers of hexagonal pores estimated from the TEM image is ca. 10 nm. The average thickness of the wall is ca. 4–5 nm and the pore diameter is around 6 nm, in agreement with the N_2 adsorption analysis (Table 1).

3.3. ^{27}Al MAS NMR

Fig. 4 shows the ^{27}Al MAS NMR spectra of the Al-SBA-15 samples. The peak at 54 ppm is ascribed to the framework aluminum species in a tetrahedral coordination. For the 30-Al-SBA-15 and 15-Al-SBA-15 samples, the absence of an ^{27}Al NMR signal at ca. 0 ppm, associated with extra framework aluminum species, confirms that aluminum is exclusively in a tetrahedral coordination. Only a weak resonance at −1 ppm (Fig. 4c) due to the presence of a small portion of extra framework octahedrally coordinated Al was observed for the 5-Al-SBA-15 sample with a high level of Al incorporation (Si/Al = 5.3). Although quantification of the total Al content in these aluminated samples by ^{27}Al NMR was complicated by the moisture content of the sample and by the magnitude of ^{27}Al quadrupolar interaction, ^{27}Al spin counting was attempted by a quantitative analysis for the 54 ppm peak intensity based on the same sample weights. The analysis showed that 5-Al-SBA-15 exhibited about two times the concentration of framework aluminum of 15-Al-SBA-15. Combined with the ICP results, about 20% of the total Al atoms in 5-Al-SBA-15 were estimated to be NMR invisible; most of them might exist as extra framework Al species. We have also tried to incorporate more Al by decreasing the Si/Al ratio down to 2.5 in the synthesis mixture. Although the ICP result was quite quantitative for the aluminated sample obtained (Si/Al = 2.4), the ^{27}Al NMR spectrum of this sample indicated that the intensities of 4- and 6-coordinated aluminum species were almost equal. Therefore, it can be concluded that the Si/Al ratio of around 5 is the maximum Al content that can be tetrahedrally incorporated via the present post-synthesis route. Interestingly, this is also the lowest Si/Al ratio that can be obtained via the direct synthesis method of pH adjustment [9]. In comparison to the post-synthesis alumination method using an aqueous solution of sodium aluminate [14], more Al was incorporated in our samples because only the Al-SBA-15 sample with an Si/Al ratio of around 20 was reported in the former case. One more advantage of the present post-synthesis route over the sodium aluminate one is that the Brønsted acidity of the Al-SBA-15 materials can be directly generated by deammoniation during thermal treatment without the need of a further ion-exchange process as in the case of sodium aluminate.

3.4. ^{19}F MAS NMR

A better understanding on the nature of the alumination process can be gained through ^{19}F MAS NMR spectroscopy

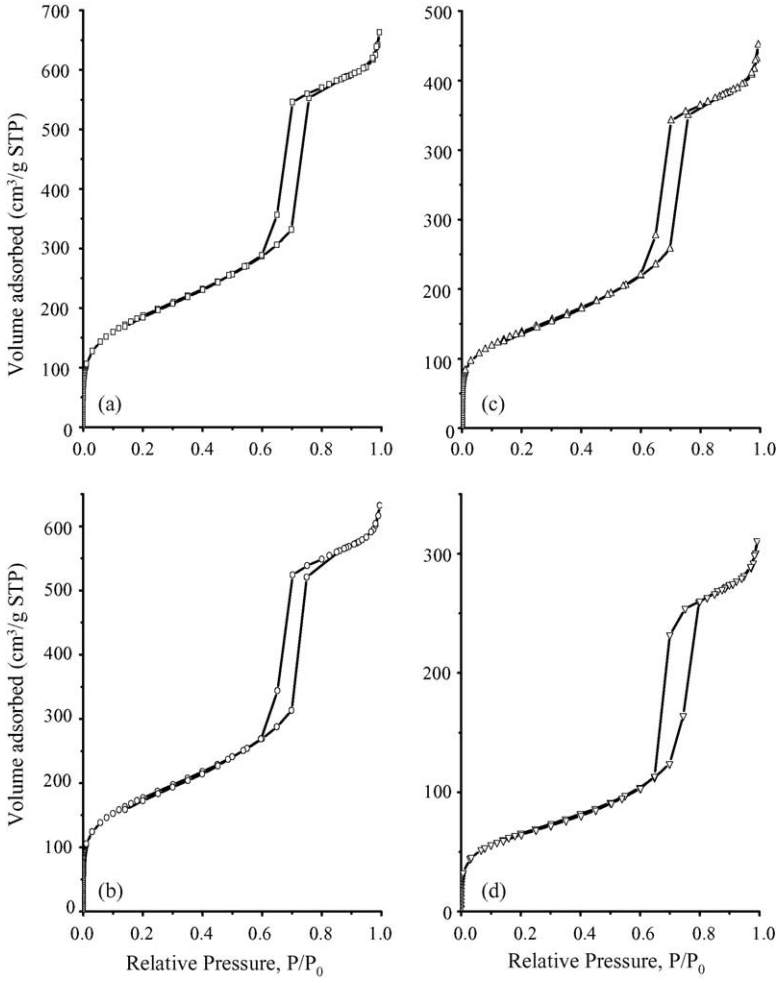

Fig. 2. N_2 adsorption–desorption isotherms of: (a) Si-SBA-15 and *x*-Al-SBA, where (b) $x = 30$, (c) $x = 15$ and (d) $x = 5$.

by examining the fluorinated species formed. Fig. 5 shows the ^{19}F MAS NMR spectra of the 15-Al-SBA-15 and 5-Al-SBA-15 samples. Only a peak at −125 ppm was observed for 15-Al-SBA-15. The broad bump underneath is due to the background signals from the probehead. The peak at −125 ppm is presumably due to the presence of the F^- counter ion of NH_4^+ in channels [20]. The poor S/N ratio of the spectrum is due to the low concentration of residual F^- ions present in the sample, possibly due to the fact that most of soluble fluoride species have been washed out during the sample preparation. For the 5-Al-SBA-15 sample, a sharp peak at −130 ppm dominated the spectrum, along with relatively broad peaks centered at −147 and −173 ppm. The peak at −130 ppm can be assigned to $(NH_4)_2SiF_6$ species, while the peaks at −147 and −173 ppm are associated with some Al–F complexes and AlF_3 species, respectively [21,22]. These two species may account for the extra framework Al species. The dominant peak at −130 ppm in the ^{19}F NMR spectrum suggests that the extracted silicon can effectively react with fluoride ions in the solution to form stable $(NH_4)_2SiF_6$ species.

3.5. $^1H/^{27}Al$ TRAPDOR NMR

Pure silica Si-SBA-15 has no Brønsted acidity. The Brønsted acidity is attributed to the formation of bridging Si(OH)Al groups, generated by the isomorphous substitution of Al for Si. A major resonance centered at 3.9 ppm with some shoulders in the range of 0.8–2.5 ppm was observed in the ^1H MAS NMR spectrum of the 5-Al-SBA-15 sample (Fig. 6a). The peak at 3.9 ppm is assigned to the protons in the Brønsted acid sites [23], indicating that the Al atom is tetrahedrally coordinated in the silica framework. The downfield shoulder centered at around 5.8 ppm is due to the residual NH_4^+ ion. The correlation between ^1H spins and ^{27}Al spins was further probed by $^1H/^{27}Al$ TRAPDOR NMR experiments in the present study. On-resonance ^{27}Al irradiation for one rotor period resulted in a significant loss of intensity of the resonance centered at 3.9 ppm (Fig. 6b), and thus a significant $^1H/^{27}Al$ TRAPDOR effect was observed as shown in the difference spectrum (Fig. 6c). The significant $^1H/^{27}Al$ TRAPDOR effect observed for the peak at 3.9 ppm confirmed that this peak was associated with bridging Si(OH)Al groups,

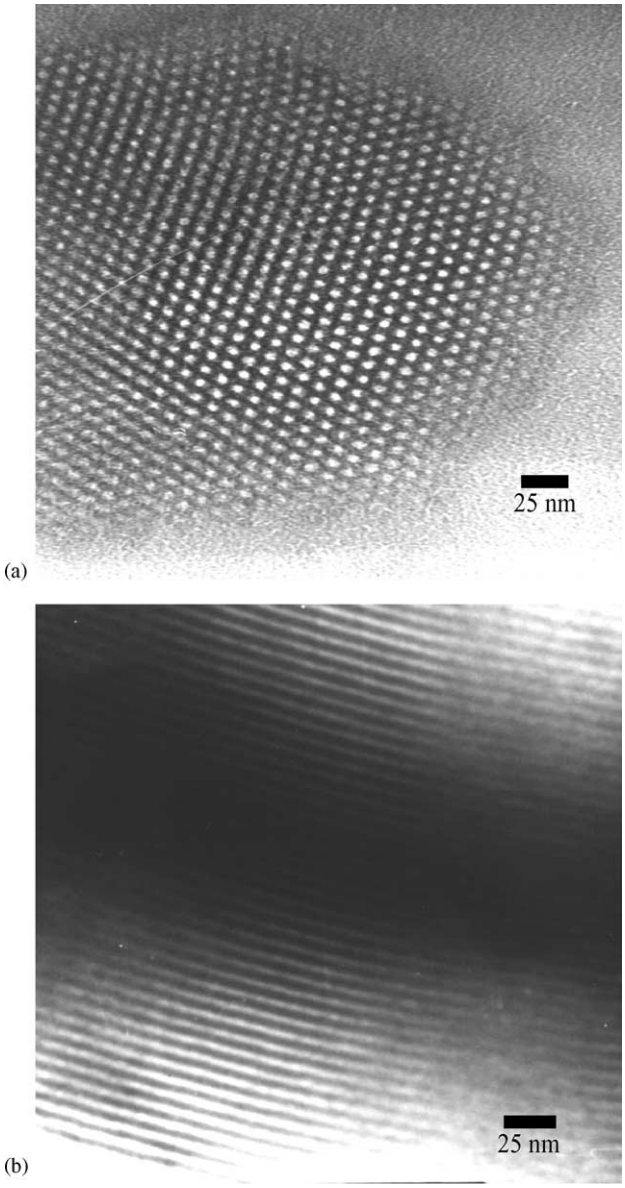

Fig. 3. TEM images of 15-Al-SBA-15: (a) in the direction of the pore axis and (b) in the direction perpendicular to the pore axis.

that is, Brønsted acidic sites. The peaks at 2.5 and 0.2 ppm can be assigned to extra framework Al-OH species, since both of them also show some TRAPDOR effects [18,23]. These extra framework Al-OH species may be associated with Lewis acid sites.

3.6. FTIR spectra of adsorbed pyridine

To evaluate the strength and types of acid sites of Al-SBA-15, pyridine adsorption measured by FTIR spectroscopy was used. Fig. 7 shows the FTIR difference spectra of Al-SBA-15, after pyridine desorption at 150 °C for 0.5 h, in the ranges 3900–3600 and 1700–1400 cm^{-1}. The band at 3740 cm^{-1} was ascribed to isolated silanol groups. All the samples with different Si/Al ratios exhibited the bands at 1545 and

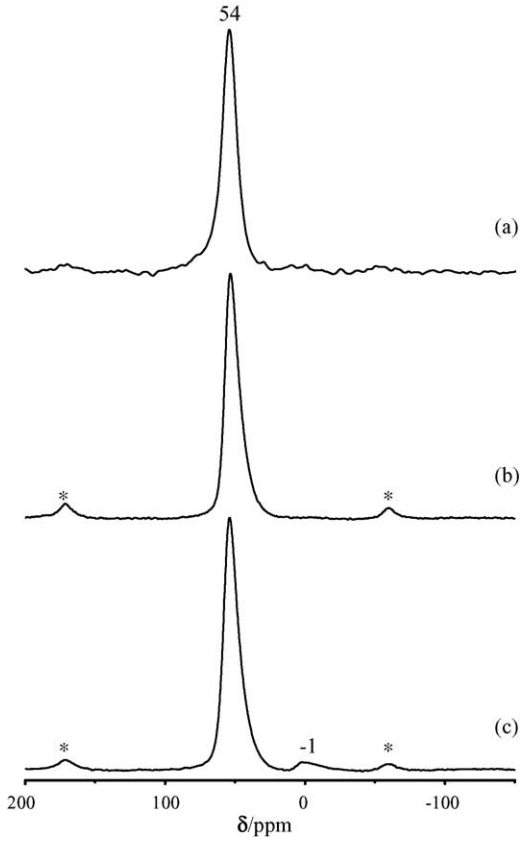

Fig. 4. ^{27}Al MAS NMR spectra of *x*-Al-SBA-15 samples, where (a) $x = 30$, (b) $x = 15$ and (c) $x = 5$, acquired at a spinning speed of 12 kHz. Asterisks denote spinning sidebands. These spectra were not normalized.

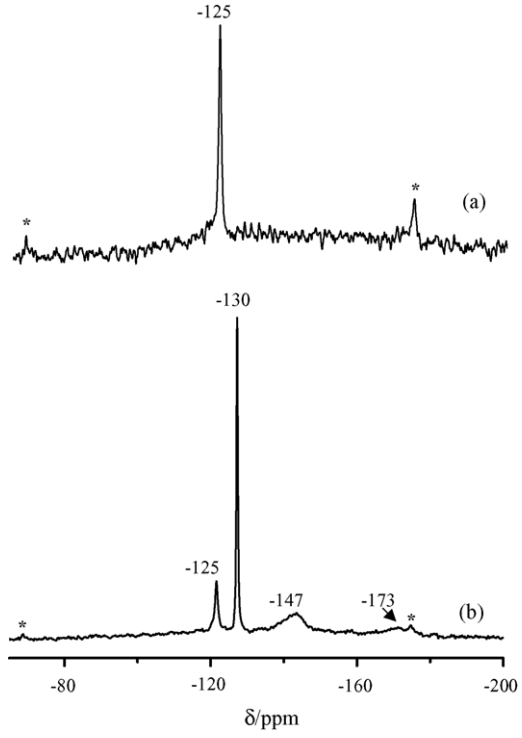

Fig. 5. ^{19}F MAS NMR spectra of: (a) 15-Al-SBA-15 and (b) 5-Al-SBA-15, acquired at a spinning speed of 20 kHz. Asterisks denote spinning sidebands.

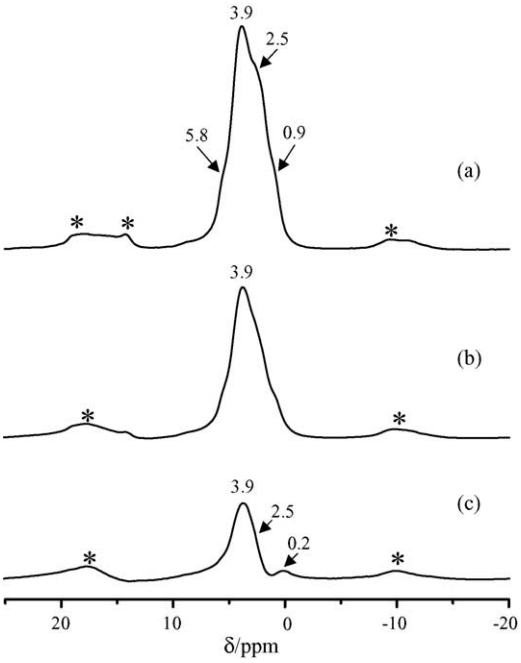

Fig. 6. $^{1}H/^{27}Al$ TRAPDOR NMR spectra of 5-Al-SBA-15: (a) without and (b) with ^{27}Al irradiation during the evolution period, τ ($\tau = 246\,\mu s$, ^{27}Al r.f. field = 50 kHz, spinning speed = 4 kHz). The difference spectrum is shown in (c). Asterisks denote spinning sidebands.

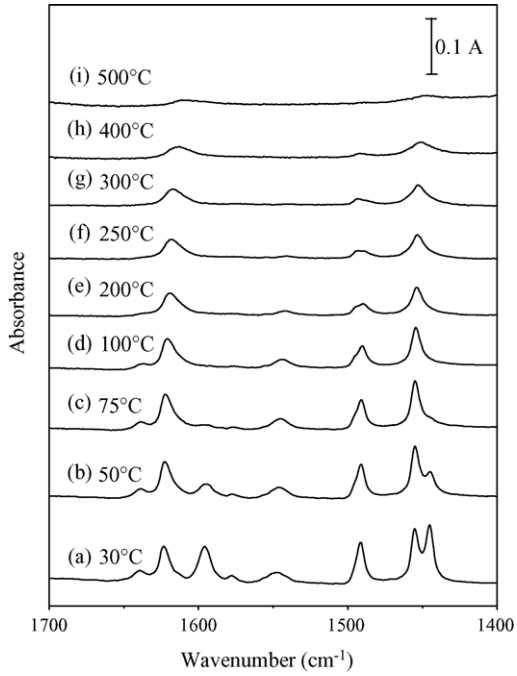

Fig. 8. FTIR spectra of the desorption of pyridine from 15-Al-SBA-15 in the temperature range 30–500 °C.

1638 cm^{-1}, and at 1454 and 1620 cm^{-1}, which are attributed to pyridine adsorbed on Brønsted acid sites and on Lewis acid sites, respectively. The band at 1490 cm^{-1} has been assigned to pyridine associated with both Brønsted and Lewis acid sites [24]. For pure silica Si-SBA-15, no signal was observed in this region on adsorption of pyridine.

The FTIR spectra of the desorption of pyridine from 15-Al-SBA-15 in the temperature range 30–500 °C, as shown in Fig. 8, were also recorded in order to estimate the strength of the acidity. The additional bands at 1445 and 1597 cm^{-1} (Fig. 8a), attributed to hydrogen-bonded pyridine, disappeared when the evacuation temperature was increased from 30 to 100 °C. With increasing evacuation temperature up to 300 °C, the band at 1454 cm^{-1} due to pyridine adsorbed on Lewis acid sites still existed, while the band at 1545 cm^{-1} due to pyridine adsorbed on Brønsted acid sites disappeared. A higher temperature above 400 °C is needed to completely remove the pyridine adsorbed on Lewis acid sites. This clearly indicates that the Lewis acidity of Al-SBA-15 is quite strong.

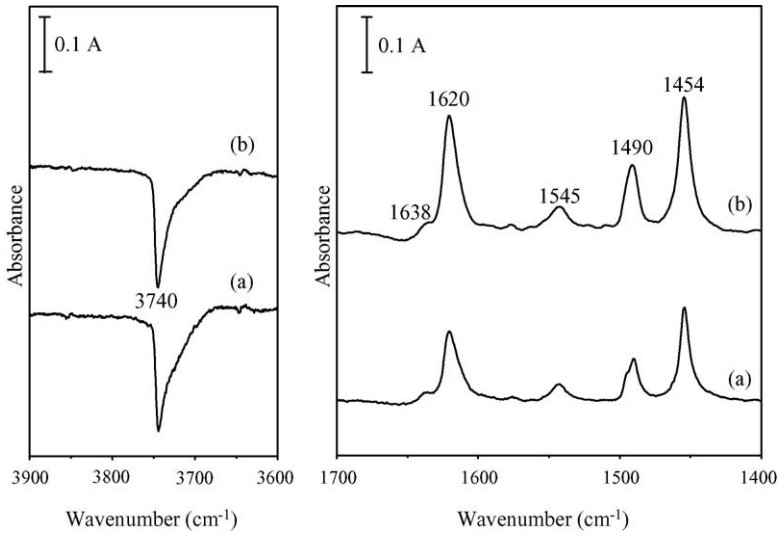

Fig. 7. FTIR difference spectra of: (a) 15-Al-SBA-15 and (b) 5-Al-SBA-15 after pyridine desorption at 150 °C for 0.5 h.

3.7. Catalytic activity

The catalytic activity of Al-SBA-15 towards cumene cracking was investigated to ascertain the acidic property. The results of the cumene cracking test on Al-SBA-15 are summarized in Table 1. The pure silica Si-SBA-15 showed no activity for cumene cracking. The Al-SBA-15 samples studied are highly active, and the activity depends strongly on the Si/Al ratio. Interestingly, the cumene conversion for 5-Al-SBA-15, which has about four times the concentration of framework aluminum of 30-Al-SBA-15 (Table 1), was only two times as high as that for 30-Al-SBA-15. This finding suggested that there would be large amounts of extra framework Al species created by the pre-treatment at 500 °C before the catalytic tests. Overall, the activity towards cumene cracking of Al-SBA-15 is higher than that of Al-MCM-41, and is comparable to that of AlPSMCM5 (Si/Al = 5) with a similar Si/Al ratio [25]. Although both SBA-15 and MCM-41 possess hexagonal mesopores, the SBA-15 structure is well known to possess complementary disordered micropores connecting the primary mesopores [26,27]. These micropores are not present in MCM-41. The micropores of Al-SBA-15 make it more resistant to pore blocking and allow faster diffusion of reactants. This may account for the higher catalytic activity of Al-SBA-15 than that of Al-MCM-41 at a similar Si/Al ratio. The high cracking activity indicates that Al-SBA-15 has the potential use in the acid-catalyzed reactions of large molecules.

3.8. pH control and possible incorporation mechanism

The adjustment of pH value of the post-synthesis mixture in the range near 9.0–9.5 is a key procedure for quantitatively incorporating Al into SBA-15 in the present synthesis route. According to the previous studies [16] and ours, ^{27}Al and ^{19}F solution NMR studies of $(NH_4)_3AlF_{6(aq)}$ as a function of pH showed that the dominant species at pH 9.3 are $Al(OH)_4^-$ (^{27}Al, $\delta = 78$ ppm) and free F^- ions (^{19}F, $\delta = -116$ ppm), respectively. The strong basic solution facilitates the hydrolysis of AlF_6^{3-} to $Al(OH)_4^-$, and thus the insertion of Al into the SBA-15 framework. Thus, it can be inferred that the mechanism for Al incorporation most likely involves the hydrolysis of AlF_6^{3-} upon basification to give $Al(OH)_4^-$ species in the first step as follows.

$$AlF_6^{3-} + 4OH^- \rightarrow Al(OH)_4^- + 6F^- \quad (1)$$

The creation of $Al(OH)_4^-$ species under basic conditions is a prerequisite for the present alumination method. The $Al(OH)_4^-$ species subsequently undergoes an isomorphous substitution for silicon in the framework walls, and the extracted silicon species react with fluoride ions to form $(NH_4)_2SiF_6$ in accordance with the following reaction.

$$\{SiO_{4/2}\} + (NH_4)_3AlF_6 \leftrightarrow \{AlO_{4/2}\}^-(NH_4)^+ + (NH_4)_2SiF_6 \quad (2)$$

where $\{SiO_{4/2}\}$ and $\{AlO_{4/2}\}^-$ refer to tetrahedral structural units containing Si and Al in the mesoporous framework, respectively. The presence of $(NH_4)_2SiF_6$ was confirmed by the prominent peak at -130 ppm in the ^{19}F MAS NMR spectrum of the 5-Al-SBA-15 sample (see Fig. 5b).

The present alumination method offers several distinct advantages. Since the NH_4^+ is potentially an acid generating cation, the Al-SBA-15 materials with Brønsted acidity can be directly obtained by deammoniation with thermal treatment. No further ion exchange would be required to create Brønsted acidity. Since the whole procedure involves an aqueous solution, no organic solvents and complicated procedures are required in contrast to other post-synthesis methods involving the use of $Al(i\text{-}OC_3H_7)_3$, $Al(CH_3)_3$ or $AlCl_3$.

4. Conclusions

In conclusion, we demonstrate that the introduction of high framework Al contents into SBA-15 can be achieved by the treatment of pure silica SBA-15 with an aqueous solution of $(NH_4)_3AlF_6$ at room temperature. The present alumination method makes it possible to retain the SBA-15 mesostructure with a low Si/Al ratio near 5. Therefore, the significance of this work includes not only providing an efficient route for synthesizing the SBA-15 with high aluminum contents, but also providing a possible strategy of using aqueous metal fluorides for making metal-containing SBA-15 heretofore difficult to prepare.

Acknowledgements

This research was supported by the National Science Council of Taiwan. Dr. Hwo-Shuenn Sheu at National Synchrotron Radiation Research Center and Dr. Chu-Hua Chien at Institute of Chemistry of Academia Sinica are gratefully acknowledged for acquiring XRD data and FTIR spectra.

References

[1] C.T. Kresge, M.E. Leonowicz, W.J. Roth, J.C. Vartuli, J.S. Beck, Nature 359 (1992) 710.
[2] D. Zhao, J. Feng, Q. Huo, N. Melosh, G.H. Fredrickson, B.F. Chmelka, G.D. Stucky, Science 279 (1998) 548.
[3] A. Corma, V. Fornés, M.T. Navarro, J. Pérez-Pariente, J. Catal. 148 (1994) 569.
[4] Z.H. Luan, H.Y. He, W.Z. Zhou, C.F. Cheng, J. Klinowski, J. Chem. Soc., Faraday Trans. 91 (1995) 2955.
[5] R. Mokaya, Chem. Commun. (2000) 1891.
[6] R. Ryoo, S. Jun, J.M. Kim, M.J. Kim, Chem. Commun. (1997) 2225.
[7] R. Mokaya, W. Jones, J. Mater. Chem. 9 (1999) 555.
[8] Y. Yue, A. Cedeon, J.L. Bonardet, N. Melosh, J.-B. D'Espinose, J. Fraissard, Chem. Commun. (1999) 1967.
[9] S. Wu, Y. Han, Y.C. Zou, J.W. Song, L. Zhao, Y. Di, S.Z. Liu, F.S. Xiao, Chem. Mater. 16 (2004) 486.
[10] Y. Li, W. Zhang, L. Zhang, Q. Yang, Z. Wei, Z. Feng, C. Li, J. Phys. Chem. B 108 (2004) 9739.

[11] (a) Y. Han, S. Wu, Y.-Y. Sun, D.-S. Li, F.-S. Xiao, Chem. Mater. 14 (2002) 1144;
(b) Y. Han, N. Li, L. Zhao, D. Li, X. Xu, S. Wu, Y. Di, C. Li, Y. Zou, Y. Yu, F.-S. Xiao, J. Phys. Chem. B 107 (2003) 7551.
[12] (a) Y. Liu, T.J. Pinnavaia, Chem. Mater. 14 (2002) 3;
(b) Y. Liu, T.J. Pinnavaia, J. Mater. Chem. 12 (2002) 3179.
[13] M. Cheng, Z. Wang, K. Sakurai, F. Kumata, T. Saito, T. Komatsu, T. Yashima, Chem. Lett. 2 (1999) 131.
[14] Z. Luan, M. Hartmann, D. Zhao, W. Zhou, L. Kevan, Chem. Mater. 11 (1999) 1621.
[15] S. Sumiya, Y. Oumi, T. Uozumi, T. Sano, J. Mater. Chem. 11 (2001) 1111.
[16] C.D. Chang, C.T.-W. Chu, J.N. Miale, R.F. Bridger, R.B. Calvert, J. Am. Chem. Soc. 106 (1984) 8143.
[17] C.P. Grey, A. Vega, J. Am. Chem. Soc. 117 (1995) 8232.
[18] H.-M. Kao, C.P. Grey, J. Phys. Chem. 100 (1996) 5105.
[19] F. Deng, Y. Yue, C. Ye, Solid State Nucl, Magn. Reson. 10 (1998) 151.
[20] L. Delmotte, M. Soulard, F. Guth, A. Seive, A. Lopez, J.L. Guth, Zeolites 10 (1990) 778.
[21] H.-M. Kao, Y.-C. Chen, J. Phys. Chem. B 107 (2003) 3367.
[22] E.C. Decanio, J.W. Bruno, V.P. Nero, J.C. Edwards, J. Catal. 140 (1993) 84.
[23] M. Hunger, Solid State Nucl., Magn. Reson. 6 (1996) 1.
[24] (a) E.P. Parris, J. Catal. 2 (1963) 371;
(b) C.A. Emeis, J. Catal. 141 (1993) 347.
[25] R. Mokaya, W. Jones, Chem. Commun. (1997) 2185.
[26] M. Impéror-Clerc, P. Davidson, A. Davidson, J. Am. Chem. Soc. 122 (2000) 11925.
[27] R. Ryoo, C.H. Ko, J. Phys. Chem. B 104 (2000) 11465.